PHYSICAL REVIEW D **79,** 083520 (2009)

Muon flux limits for Majorana dark matter from strong coupling theories

Konstantin Belotsky,[1] Maxim Khlopov,[1,2] and Chris Kouvaris[3]

[1]*Moscow Engineering Physics Institute, Moscow, Russia and Center for Cosmoparticle Physics, "Cosmion," Moscow, Russia*

[2]*APC Laboratory, Paris, France*

[3]*The Niels Bohr Institute, Copenhagen, Denmark*

(Received 1 November 2008; published 16 April 2009)

We analyze the effects of the capture of dark matter (DM) particles, with successive annihilations, predicted in the minimal walking technicolor model (MWT) by the Sun and the Earth. We show that the Super-Kamiokande upper limit on excessive muon flux disfavors the mass interval between 100 and 200 GeV for MWT DM with a suppressed standard model interaction (due to a mixing angle), and the mass interval between 0 and 1500 GeV for MWT DM without such suppression, upon making the standard assumption about the value of the local DM distribution. In the first case, the exclusion interval is found to be very sensitive to the DM distribution parameters and can vanish at the extreme of the acceptable values.

DOI: 10.1103/PhysRevD.79.083520 PACS numbers: 95.35.+d, 12.60.Nz

I. INTRODUCTION

The possibility of breaking the electroweak symmetry in a natural dynamical way in the context of technicolor has been very appealing since it was first introduced in the 1970s [1,2]. It was soon realized that in order to overcome the problems of the first models, and, in particular, the necessity to give mass even to the heaviest standard model particles like the top quark, a walking coupling is required. However, such a quasiconformal behavior was associated with a large number of extra flavors coupled to the electroweak sector, making it impossible to evade the strict constraints from the electroweak precision measurements. Recently, in a series of papers [3–6], it has been demonstrated that the above problem can be avoided as soon as the techniquarks transform under higher dimensional representations of the gauge group. More specifically, theories with fermions in the two-index symmetric representation of the gauge group can accommodate such a quasiconformal behavior with a very small number of flavors, in contrast to the case where the fermions transform under the fundamental representation. This set of theories does not violate the experimental constraints, thus being an eligible candidate for the upcoming search of the LHC.

Since, in principle, such theories are strongly coupled, a perturbative treatment can offer very little. Nonperturbative techniques and tools should be implemented for the exploration and study of these theories. In this context, the first lattice simulations have been developed [7–9]. Similarly, low energy effective theories, valid at the scale where the LHC will operate, can offer an alternative approach to the problem, as well as distinct signatures that can rule in or rule out walking technicolor (WTC) models [10–12]. In addition, holographic methods inspired by the AdS/CFT correspondence can reduce the parameter space of the arbitrary couplings of the effective theories and make more definite phenomenological predictions [13,14]. This last idea is quite promising, especially if one takes into consideration the fact that quasiconformal theories resemble the exact conformal $N = 4$ theory more than QCD, where this method has given results close to the known experimental values.

The simplest of the WTC models is the one with only two flavors in the technicolor sector, i.e. the techniquarks U and D, where they transform under the two-index symmetric representation of an $SU(2)$ gauge group.[1] There is an extra family of heavy leptons, i.e. ν' and ζ, that couple to the electroweak sector, in order to cancel the Witten global anomaly [10]. Such a theory, although simple in terms of particle content, has a very rich structure. The techniquarks possess an enhanced $SU(4)$ global symmetry that includes $SU(2)_L \times SU(2)_R$ as a subgroup. This is due to the fact that the adjoint representation is real. After chiral symmetry breaking, the vacuum is invariant under an $SO(4)$ symmetry that includes the $SU(2)_V$ as a subgroup. Nine Goldstone bosons emerge from the breaking, three of which are eaten by the W and Z bosons. The remaining six bosons come in three particle-antiparticle pairs, and are UU, UD, and DD, where we have suppressed color and Dirac indices. Their main feature is that, although they are Goldstone bosons, they are not regular mesons, like the pions, since they are composed of two techniquarks, rather than a quark-antiquark pair. Therefore these Goldstone bosons carry technibaryon number that can protect the lightest particle from decaying. This fact opens interesting possibilities for dark matter (DM) candidates.

There is an anomalous-free hypercharge assignment for the techniquarks, which makes one of them electrically neutral. For the sake of our study, we choose D to be the one, although the results are identical if we make U neutral instead of D. For the above hypercharge assignment, the

[1]The two-index representation of the $SU(2)$ is the adjoint one.

corresponding electric charges are $U = 1$, $D = 0$, $\nu = -1$, and $\zeta = -2$. The first possibility of having a dark matter candidate is the case where the DD (which is electrically neutral) is also the lightest technibaryon [15]. The technibaryon number of DD can protect it from decaying to standard model particles, as long as there are no processes that violate the technibaryon number below some scale. The sphaleron processes violate the technibaryon number; however, they become ineffective once the temperature of the Universe drops below the electroweak scale. Such a particle can account for the whole dark matter density, as long as its mass is of order TeV. However, such a scenario is excluded by direct dark matter search experiments, since the cross section of DD scattering off nuclei targets is sufficiently large and should be detected in these experiments. This problem can be avoided in a slightly different version of the MWT [16]. Another possibility is to assume that UU is the lightest technibaryon. In this case, it is possible to form electrically bound neutral states between $^4\mathrm{He}^{++}$ and $\bar{U}\bar{U}$ [17–19]. Alternatively, $^4\mathrm{He}^{++}$ can be bound to ζ^{--}. This scenario cannot be excluded by underground detectors, and therefore, it is a viable candidate.

In this paper we focus on yet a third possibility. Because of the fact that in WTC the techniquarks transform under the adjoint representation of the gauge group, it is possible to form bound states between a D and technigluons [20]. The object D^aG^a, where G represents the gluons of the theory and a runs over the three color states (since it is the adjoint representation), is electrically neutral and colorless. If D_LG has a Majorana mass, a seesaw mechanism is implemented and the mass eigenstates are two Majorana particles, namely, a heavy N_1 and a light N_2. Although the Majorana mass term breaks the technibaryon symmetry, a Z_2 symmetry, like the R parity in neutralinos, protects N_2 from decaying. Because N_2 is a linear combination of D_LG and D_RG (which has no electroweak coupling), N_2 has a suppressed coupling to the Z boson of the form

$$\frac{\sqrt{g^2 + g'^2}}{2} Z_\mu \sin^2\theta \bar{N}_2 \gamma^5 \gamma^\mu N_2, \tag{1}$$

where g and g' are the electroweak and hypercharge couplings, respectively. We have omitted terms that couple N_1 with N_2, as N_1 is very heavy and decays to N_2 very fast. The mixing angle θ is defined through the relation $\tan 2\theta = 2m_D/M$, where m_D and M are the Dirac and Majorana masses of the D_LG particle. Although the Z_2 symmetry can protect N_2 from decaying, two N_2 can coannihilate to standard model particles through Z boson mediation. For small masses of N_2, the main annihilation channel in the early Universe is to light particle-antiparticle pairs, like quarks and leptons. For larger masses, the dominant channel is annihilation to pairs of $W^+ - W^-$. It was shown in [20] that because of the $\sin\theta$ dependence of the annihilation cross section, $\sin\theta$ can be chosen accordingly in such a way that the relic density of N_2 matches the dark matter density of the Universe. This is depicted in Fig. 1, where $\sin\theta$ is given as a function of the mass of N_2, in order for N_2 to account for the dark matter density. The fact that N_2 is a Majorana particle and consequently does not have coherent enhancement in scattering off the nuclei targets in the underground detectors, along with the suppression of the cross section that scales as $\sin^4\theta$, makes N_2 evasive from experiments like the Cryogenic Dark Matter Search (CDMS) for almost any mass of interest. For the same reason, this form of dark matter cannot explain the positive results of DAMA/NaI and DAMA/Libra experiments [21]. Under specific conditions, N_2 can be excluded as a main dark matter particle only for a small window of masses, roughly between 100 and 150 GeV [22]. N_2 is also susceptible to indirect signatures such as those suggested in [23].

In a similar fashion, for a hypercharge assignment where ν' is neutral, this heavy neutrino can be a dark matter particle if the evolution in the early Universe is dominated by quintessence-like dark energy [24]. However, it was pointed out in [22] that such a candidate, even in the case where ν' is a Majorana particle, is excluded for masses up to 1 TeV (depending on the value of the local dark matter density of the Earth).

We should emphasize here that the investigation and the results of [20] can also apply to ν' when it is electrically neutral, if we assume that the left-handed ν' has a Majorana mass and a Dirac mass. Because of the fact that DG (for the hypercharge value that makes it neutral) interacts with the electroweak sector as ν' does (for a different hypercharge that makes ν' neutral), N_2 can equally represent the lightest Majorana particle made of DG or ν'.

We would like to stress a few points regarding the models we use in this paper. By now, it has been established in a solid way that only quasiconformal technicolor theories can pass the electroweak precision tests and simultaneously avoid the problems of old technicolor theories (like the large effect of flavor changing neutral current). To our knowledge, the technicolor models we examine are the only viable technicolor models that are not excluded and also have desired features (light Higgs, stable DM, etc.). The model that we have focused on, the

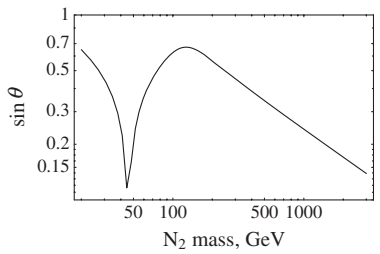

FIG. 1. Dependence of the mixing parameter $\sin\theta$ on the mass of N_2.

MWT model, is the simplest of all and is comprised of two techniquarks in the adjoint of $SU(2)$. Our analysis is valid for the general case of technicolor dark matter models that are not based on the stability of technibaryon number or on the excess of particles over antiparticles.

The paper is organized as follows: In Sec. II, we calculate the relevant annihilation cross sections for the early Universe and the Sun. In Sec. III, we calculate the capture rate of the relic density by the Sun and the Earth. In Sec. IV, we provide the muon flux from the captured dark matter particles. We present our conclusions, and a discussion of the uncertainties that might enter in our results, in Sec. V.

II. ANNIHILATION OF N_2 IN THE EARLY UNIVERSE AND IN THE SUN

A pair of N_2 annihilates mainly into pairs of fermions, $f\bar{f}$, and into pairs of W bosons, W^+W^- (with longitudinal polarization), provided that the energy is sufficient to open the corresponding channel. In our calculation we adopt the following formulas for the annihilation cross sections multiplied by the relative velocity and averaged over the thermal velocity distribution at temperature T,

$$\langle\sigma v\rangle_{ff} = \frac{2G_F^2 m^2 \beta_f}{\pi} P_Z \left\{ \frac{C_A^2}{2}\frac{m_f^2}{m^2} + \left[(C_V^2 + C_A^2) + \left(\frac{C_V^2}{2} - \frac{17C_A^2}{8} \right) \frac{m_f^2}{m^2} \right] \frac{T}{m} \right\} \sin^4\theta, \tag{2}$$

$$\langle\sigma v\rangle_{WW} = \frac{2G_F^2 m^2 (2m^2 - m_W^2)^2 \beta_W^3}{\pi m_Z^4} P_Z \frac{T}{m} \sin^4\theta, \tag{3}$$

which are deduced from [20,24–26]. Here

$$P_Z = \frac{m_Z^4}{(4m^2 - m_Z^2)^2 + \Gamma_Z^2 m_Z^2}, \qquad \beta_{f,W} = \sqrt{1 - m_{f,W}^2/m^2},$$

where m_f, m_Z, m_W, and m are the masses of the final fermion f, Z and W bosons, and N_2, respectively; G_F is the Fermi constant; $C_V = T_{3L} - 2Q\sin^2\theta_W$; and $C_A = T_{3L}$ are standard model parameters of f. T_{3L} and Q are the weak isospin and the electric charge of the corresponding particle. Equations (2) and (3) represent the cross sections in a nonrelativistic approximation in the form of

$$\langle\sigma v\rangle = \sigma_0 + \sigma_1 \frac{T}{m}. \tag{4}$$

In the standard big bang scenario, the modern relic density of N_2 is given by [20]

$$\Omega_{N_2} h^2 = \frac{1.76 \times 10^{-10} \sqrt{g_*}}{g_{*s} \sigma_1 [\mathrm{GeV}^{-2}]} \left(\frac{m}{T_*} \right)^2, \tag{5}$$

where the freeze-out temperature is given by

$$\frac{m}{T_*} = L - \frac{3}{2}\ln[L], \qquad L = \ln\left[\frac{m_{\mathrm{Pl}} m \sigma_1}{6.5\sqrt{g_*}} \right]. \tag{6}$$

m_{Pl} is the Planck mass, and g_* and g_{*s} are effective spin degrees of freedom contributing to the energy and entropy densities of the plasma at $T = T_*$, respectively. For the T_* values of interest, $g_* = g_{*s} = 80 \div 100$.

By inspection of Eqs. (2) and (3), we see that at the freeze-out, the cross section is dominated by $\langle\sigma v\rangle = \sigma_1 \cdot T/m$ for all the annihilation channels ($N_2N_2 \to WW$, $N_2N_2 \to f\bar{f}$, with f being $\nu_{e,\mu,\tau}$, e, μ, τ, u, d, s, c, b). For the annihilation of N_2 into top-quark-antiquark pairs, the first term of Eq. (4) can be important (for the mass

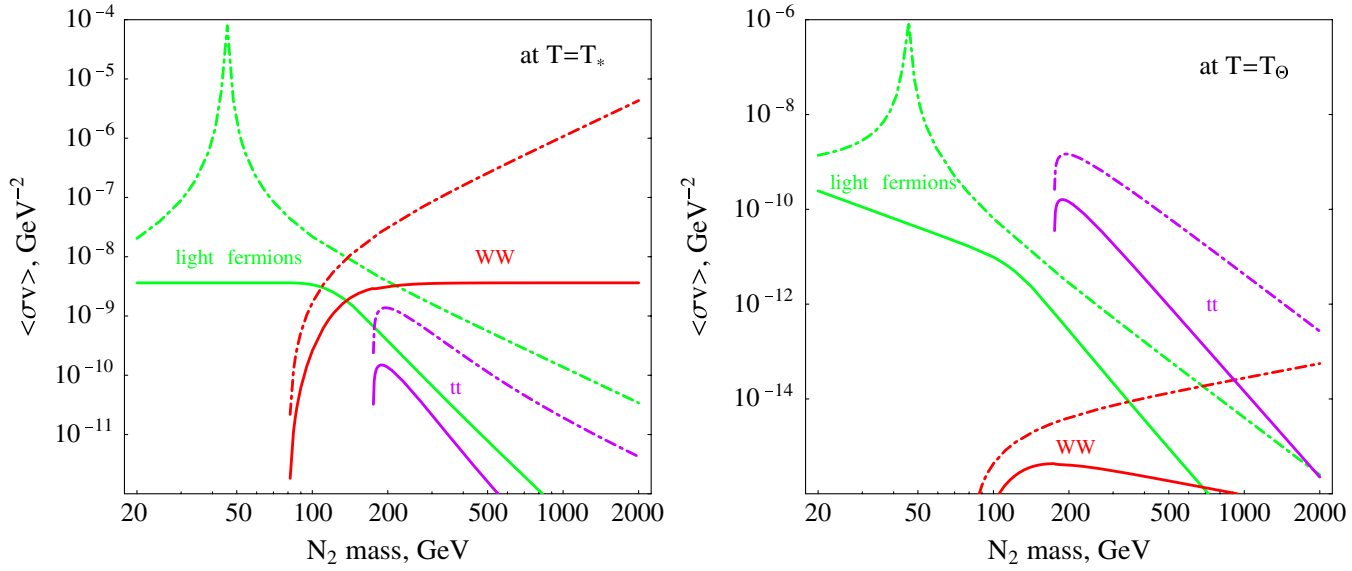

FIG. 2 (color online). The cross sections of $N_2N_2 \to$ light fermions, $t\bar{t}$, WW are shown for the models from [20] (solid lines) and [24] (dot-dashed lines) at freeze-out (left panel) and for the Sun (right panel). "Light fermions" include all fermions except the top quark; channels with off-mass shell W or f were not taken into account.

interval $m_t < m \lesssim 500$ GeV); however, for $m > m_t$, the WW channel strongly prevails during the freeze-out period.

The condition that N_2 saturates all the cold dark matter (CDM),

$$\Omega_{N_2} h^2 = \Omega_{\rm CDM} h^2 = 0.112, \tag{7}$$

fixes the free parameter of the model $\sin\theta$ [or σ_1 in Eqs. (5) and (6)]. It is given in Fig. 1 as a function of the mass of N_2. In the model of pure Majorana neutrinos (i.e. ν') [24], where $\sin\theta = 1$, such a condition is provided by an extension of the big bang scenario due to quintessence [27]. Because of this, there is a difference between the annihilation cross sections predicted in these two variants of MWT DM particles, as shown on Fig. 2 (left panel). In the model from [20], the total cross section at the freeze-out is virtually independent of the mass due to the fact that it is always adjusted via Eq. (7) in order to give the proper relic density. However, at the temperatures of the solar core, $T_\odot \approx 1.3$ keV $\ll T_*$, the first term in Eq. (4) [or Eq. (2)] dominates for many types of final fermions. Therefore, annihilation rates inside the Sun are different from those in the early Universe (see Fig. 2, right panel). Channels with light final fermions in the Sun become suppressed with respect to those in the early Universe, while the $t\bar{t}$ channel becomes of special importance (see Sec. IV).

III. CAPTURE OF RELIC N_2 BY THE SUN AND THE EARTH

Relic N_2 with density in the vicinity of the Solar System, assumed to be $\rho_{\rm loc} = 0.3$ GeV/cm^3, may scatter off nuclei inside the Sun and the Earth and can be trapped by their corresponding gravitational potential wells. The interaction of N_2 with nuclei A is spin dependent and the respective cross section can be represented as [20]

$$\sigma_{N_2 A} = \frac{2 G_F^2 \mu^2}{\pi} I_s \sin^4\theta, \tag{8}$$

where μ is the reduced mass of N_2 and A, and

$$I_s = C^2 \cdot \lambda^2 J(J+1). \tag{9}$$

The coefficient C takes into account quark contributions to the spin of the nucleon, and for weak interactions it is [28,29]

$$C = \sum_{q=u,d,s} T_{3q} \Delta q \approx \begin{cases} \frac{1}{2}0.78 - \frac{1}{2}(-0.48) - \frac{1}{2}(-0.15) = 0.705 & \text{for } p \\ \frac{1}{2}(-0.48) - \frac{1}{2}0.78 - \frac{1}{2}(-0.15) = -0.555 & \text{for } n. \end{cases} \tag{10}$$

The other coefficient in Eq. (9) relates the nucleon contribution (with spin s and orbital momentum l) to the spin J of the nucleus, and within the single unpaired nucleon model, it is

$$\lambda^2 J(J+1) = \frac{[J(J+1) + s(s+1) - l(l+1)]^2}{4J(J+1)}. \tag{11}$$

We assume that only hydrogen contributes to the capture of relic N_2 in the Sun. In this case, from Eqs. (9)–(11) we have $I_s = 0.705 \cdot \frac{3}{4} \approx 0.37$. This estimate agrees with that for Dirac neutrinos, taking into account only the axial current (spin-dependent) contribution, which gives [30] $I_s \approx 1.3^2 \cdot 3/16 \approx 0.3$. The case of the Earth will be commented separately.

It is not difficult to estimate the capture rate of the Sun or the Earth. The common expression for that is

$$\dot{N}_{\rm capt} = \sum_A \int n_{N_2} \langle \sigma'_{N_2 A} v \rangle n_A dV, \tag{12}$$

where n_{N_2} and n_A are the number densities of N_2 and A in a given volume element dV, and $\sigma'_{N_2 A}$ is the cross section for an $N_2 - A$ collision times the probability that N_2 loses enough energy to be gravitationally trapped by the Sun. Introducing a nuclear form factor F_A, one writes

$$\sigma'_{N_2 A} = \sigma_{N_2 A} \int_{T_\infty}^{\Delta T_{\rm max}} F_A^2(\Delta T) \frac{d\Delta T}{\Delta T_{\rm max}} = \sigma_{N_2 A} \bar{F}_A^2 \frac{v_{\rm esc}^2(r) - \delta v_\infty^2}{v^2}, \tag{13}$$

where ΔT is the transferred energy in an $N_2 - A$ collision, $\Delta T_{\rm max} = 2\mu^2 v^2 / m_A$, $\delta = (m - m_A)^2/(4 m m_A)$ with m_A being the nucleus mass, $v_{\rm esc}$ is the escape velocity at distance r from the center of gravity, and $v = \sqrt{v_\infty^2 + v_{\rm esc}^2}$ and v_∞ are the N_2 velocities at distances r and $r \to \infty$, respectively. $\bar{F}_A^2$ is the F_A^2 averaged over the interval $\Delta T \in [T_\infty; \Delta T_{\rm max}]$, where $T_\infty \equiv m v_\infty^2/2$. The number density n_{N_2} of N_2 at distance r can be related to the one outside the potential well, $n_{N_2}(r \to \infty) \equiv n_{N_2 \infty}$, as [30,31] $n_{N_2} = n_{N_2 \infty} \cdot v / v_\infty$. We average Eq. (12) over the velocity distribution, by the substitution

$$n_{N_2 \infty} \to n_{N_2 \infty} \cdot f_\infty(v_\infty) dv_\infty,$$

where $n_{N_2 \infty} = \rho_{\rm loc}/m$. We use a velocity distribution of the form

$$f_\infty(v_\infty) = \frac{v_\infty}{\sqrt{\pi} v_0 v_\odot} \left(\exp\left[-\frac{(v_\infty - v_\odot)^2}{v_0^2} \right] - \exp\left[-\frac{(v_\infty + v_\odot)^2}{v_0^2} \right] \right), \tag{14}$$

where $v_\odot = v_0 = 220$ km/s. The captured N_2 accumulate in the solar core and annihilate. Their number density is governed by the equation

$$\dot{N} = \dot{N}_{\rm capt} - \dot{N}_{\rm ann}. \tag{15}$$

Here, $\dot{N}_{\rm ann}$ is the number of N_2 disappearing due to annihilation per second,

$$\dot{N}_{\rm ann} = \int n_{N_2}^2 \langle \sigma v \rangle dV.$$

It is 2 times larger than the rate of annihilation acts. The effect of evaporation of the captured and thermalized N_2 is neglected, something that is valid for all $m \gtrsim 3$ GeV [26]. Thermalization of the captured N_2 happens, due to succession of collisions with nuclei, well before N_2 has time to annihilate (the ratio of respective characteristic times, within N_2 mass range of interest, is $\sim 10^{-5 \div -10}$ for the Sun). Resolving Eq. (15) for $\dot{N}_{\rm ann}$, one finds

$$\dot{N}_{\rm ann} = \dot{N}_{\rm capt} \tanh^2\left[\sqrt{\frac{\dot{N}_{\rm capt}}{\dot{N}_{\rm eq}}}\right].$$

Here

$$\dot{N}_{\rm eq} = \frac{V_{\rm therm}}{\langle \sigma v \rangle t_{\rm age}^2}$$

defines a critical capture rate above which equilibrium between capture and annihilation is established during the solar lifetime $t_{\rm age}$. For $\dot{N}_{\rm capt} \ll \dot{N}_{\rm eq}$, $\dot{N}_{\rm ann}$ is suppressed with respect to $\dot{N}_{\rm capt}$ as $\dot{N}_{\rm capt}/\dot{N}_{\rm eq}$. The value

$$V_{\rm therm} = \left(\frac{4\pi\bar{\rho}}{\rho_{\rm core}}\frac{T_{\rm core}}{T_{\rm esc}}\right)^{3/2} R^3 \approx \left(\frac{\rm TeV}{m}\right)^{3/2} \begin{cases} 2.0\times 10^{26}\ {\rm cm}^3 \left(\frac{T_{\rm core}}{15\times 10^6\ {\rm K}}\right)^{3/2}\left(\frac{150\ {\rm g/cm^3}}{\rho_{\rm core}}\right)^{3/2} & \text{for the Sun} \\ 1.0\times 10^{23}\ {\rm cm}^3 \left(\frac{T_{\rm core}}{7000\ {\rm K}}\right)^{3/2}\left(\frac{11\ {\rm g/cm^3}}{\rho_{\rm core}}\right)^{3/2} & \text{for the Earth} \end{cases} \quad (16)$$

characterizes the effective volume that the captured N_2 occupy, after being thermalized, having a Maxwell-Boltzmann velocity distribution. Here, R is the radius of the Sun or the Earth; $\bar{\rho}$, $\rho_{\rm core}$, and $T_{\rm core}$ are their mean and core densities and core temperatures, respectively (for the Sun $T_{\rm core} \equiv T_\odot$), and $T_{\rm esc} \equiv m v_{\rm esc}^2(r=R)/2$. For the derivation of Eq. (16) we assume that the density of matter and the temperature within $V_{\rm therm}$ are constant and equal to their core values. In this case, the potential energy with respect to the center takes the form $U(r) = T_{\rm esc}(\rho_{\rm core}/\bar{\rho}) \times (r/R)^2/2$, and an integration of the thermalized N_2 number density, $n_{N_2}(r) = n_{N_2}(0)\exp(-U(r)/T_{\rm core})$, can be done analytically. Note that the quantity given in Eq. (16) for the Sun agrees with the one in [32]. For the integration in Eq. (12), we assume a matter density distribution in r as in [30]. The effect of the finite size of hydrogen is insignificant in this case. In fact, $qa < 0.1$ (typically ~ 0.02), where $q = \sqrt{2 m_A \Delta T}$ is the transferred three-momentum and a is the nucleus size, so $F_A(qa) \approx 1$. The capture and annihilation rates obtained for the case of the Sun are shown in Fig. 3. For comparison, the same results obtained within the approximation of [33,34]

$$\dot{N}_{\rm capt} \approx 4.5\times 10^{18}\ {\rm s}\cdot \frac{\rho_{\rm loc}}{0.4\ {\rm GeV/cm^3}}\left(\frac{270\ {\rm km/s}}{\bar{v}}\right)^3 \times \frac{\sigma_{H,SD}}{10^{-6}\ {\rm pb}}\left(\frac{1000\ {\rm GeV}}{m}\right)^2$$

are shown in Fig. 3, too. As seen, the agreement is very good.

As for the capture by the Earth, the essential difference is that the potential well in this case is very "shallow," and incident DM particles have a chance of being captured only under special kinematic conditions. This may happen in scattering off nuclei with nonzero spin, if the DM particle has a mass close to the mass of the nucleus and/or it is initially very slow. As a rough estimate, we take one of the nuclei with nonzero spin that is quite abundant in the Earth: the isotope ^{57}Fe present in natural Fe with a fraction $\approx 2\%$, while all iron is assumed to make up $\approx 30\% \div 40\%$ of the

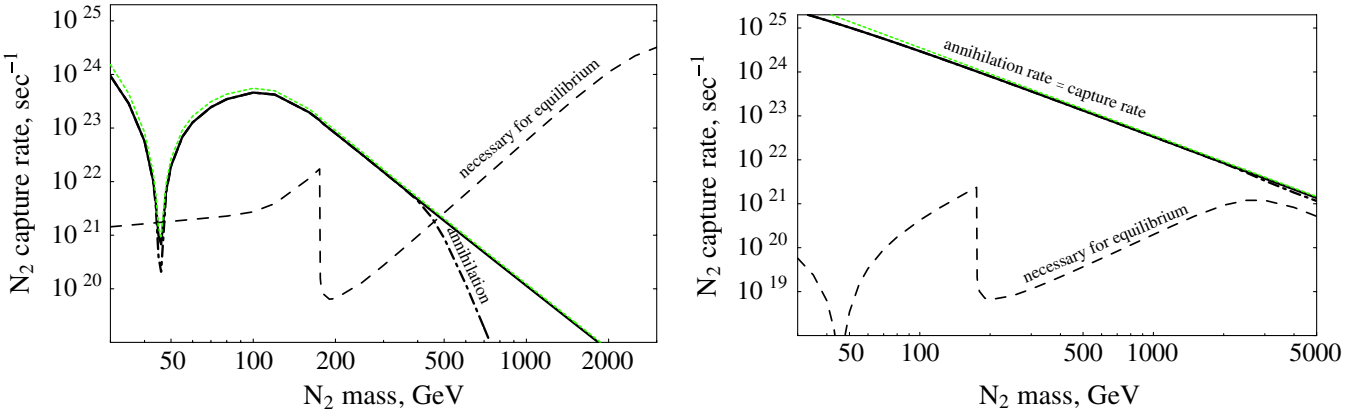

FIG. 3 (color online). The capture and annihilation rates for N_2 in the case of the Sun for the models from [20] (left panel) and [24] (right panel). Dotted (green) lines show the capture rates obtained in the approximation [33,34].

Earth's mass. We assume that it is concentrated in the core of the Earth. In the core, $v_{\rm esc}(r \approx 0) \approx 14.2$ km/s. The cross section of the $^{57}\mathrm{Fe} - N_2$ interaction is defined in Eq. (8). For I_s, one can give a maximal estimate in the single unpaired nucleon approximation of $I_s \approx 0.23$ [from Eqs. (9)–(11)]. The form factor of iron can be roughly estimated in the thin sphere approximation [28],

$$F_A(qa) = \frac{\sin(qa)}{qa}.$$

Since the integration interval in Eq. (13) is small (in the case of the Earth) with respect to the characteristic scale of the F_A variation, we take $\bar{F}_A^2 = F_A^2(T_\infty)$. For a simple (maximal) estimate, we use Eq. (14) as the N_2 distribution in the vicinity of the Earth, where the depletion in the v space for $v < 42$ km/s caused by solar attraction is ignored (moreover, we also neglect the effect of possible accumulation of dark matter particles in the Solar System, described in [35]). The capture rates of the Earth's potential due to $^{57}\mathrm{Fe} - N_2$ collisions as obtained for the two MWT models considered are represented in Fig. 4. As seen in Figs. 3 and 4, in the model from [20], $\dot{N}_{\rm capt}$ is lower and $\dot{N}_{\rm eq}$ is higher (compared to the other model considered), which is a consequence of the $\sin^4\theta$ suppression of both N_2N_2 and $A - N_2$ interactions [Eqs. (2), (3), and (8)]. In the case of the Earth, the annihilation channel $N_2N_2 \to WW$ is suppressed with respect to the case of the Sun by $7000\ \mathrm{K}/15 \times 10^6\ \mathrm{K} \sim 5 \times 10^{-4}$, and therefore $\dot{N}_{\rm eq}$ in Fig. 4 does not fall for $m \gtrsim 2$ TeV. Similarly, neutrino yields from annihilation in the Earth and the Sun should not differ for $m \lesssim 2$ TeV, except for a difference caused by absorption effects in the solar matter, being meaningful only for high N_2 masses.

By comparison of Figs. 3 and 4, we see that for the maxima of $\dot{N}_{\rm capt}$ in the case of the Earth, which occur for a mass of N_2 close to the mass of ^{57}Fe, the ratio of $\dot{N}_{\rm capt}$ for the Earth over the Sun is $\sim 10^{-10}$ in both models considered [20,24]. The neutrino flux, induced by annihilation of N_2 in the Earth, will differ from that from the Sun as the aforementioned ratio multiplied by the squared ratio of distances to the Sun and the Earth centers 5×10^8 and a factor $\dot{N}_{\rm capt}/\dot{N}_{\rm eq} \sim 10^{-4}$ for the model from [20]. So, even for the model from [24], where the $\dot{N}_{\rm capt}/\dot{N}_{\rm eq}$ suppression is much weaker, the N_2-annihilation-induced neutrino flux from the Earth at its maximum is a few tens times less than that from the Sun. A greater neutrino flux from the Earth relative to that from the Sun can hardly be expected from collisions of relic N_2 with other nuclei present in the Earth, for which the abundance is more uncertain. Since the sensitivity of the Super-Kamiokande (SK) experiment to the neutrino induced muon flux from both the solar and Earth cores is of the same order of magnitude, we shall neglect N_2 annihilation effects in the Earth in the following consideration.

IV. MUON FLUX FROM THE CAPTURED N_2

Annihilation of N_2 produces e, μ, and τ neutrinos with a flux

$$\Phi_\nu = \dot{N}_{\rm ann} \frac{N_\nu}{2 \cdot 4\pi r^2},$$

where N_ν is the multiplicity of neutrinos produced per N_2N_2 annihilation, and r is the distance to the center of the Sun or the Earth. Neutrinos from annihilation passing through the solar matter can reach the Earth, traverse it, and induce at its surface the muon flux

$$\Phi_\mu = \Phi_{\nu_\mu} \frac{x_\mu}{x_{\nu_\mu}} = \frac{\dot{N}_{\rm ann}}{2 \cdot 4\pi r^2} \int dN_{\nu_\mu}(E_{\nu_\mu}) \frac{\langle x_\mu \rangle}{x_{\nu_\mu}} \qquad (17)$$

where x_μ and x_{ν_μ} are the mean free paths (measured as matter columns in g/cm^2) of μ and ν_μ with respect to the processes of energy loss (mainly ionization) and $\nu_\mu + A \to \mu + X$. The last equality in Eq. (17) is a generalization for the case of energy dependence.

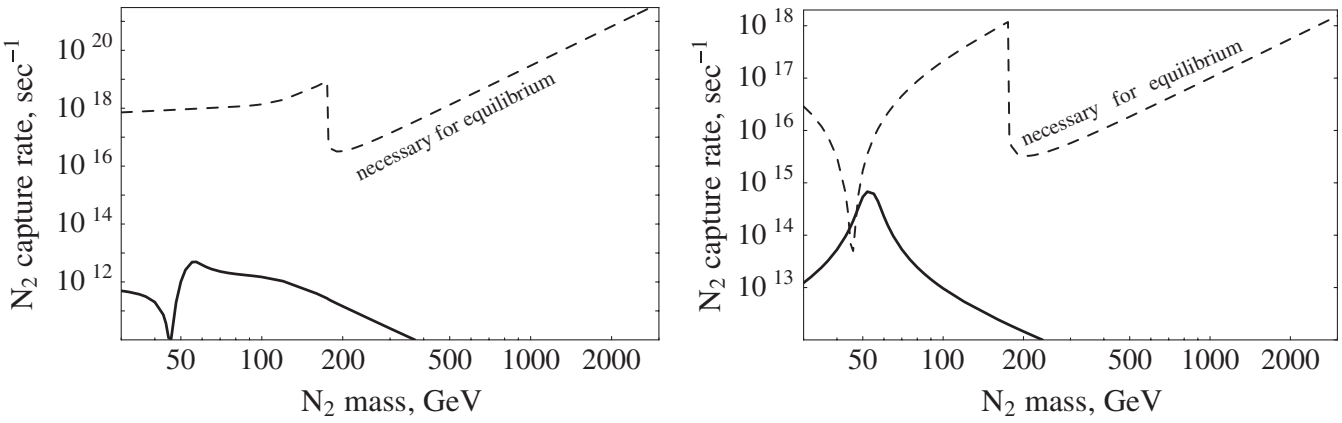

FIG. 4. A rough estimate of the capture rates of relic N_2 by the Earth for the models from [20] (left panel) and [24] (right panel).

For muon energy losses we use the approximation [36]

$$-\frac{dE_\mu}{dx_\mu} = a \approx 2.3\frac{\text{MeV}}{\text{g/cm}^2}, \tag{18}$$

taking into account ionization effects and ignoring pair production and bremsstrahlung effects. This approximation is valid for $E_\mu \lesssim 800$ GeV and seems reasonable within the energy interval of concern, as will be seen from the final result. The muon mean free path is

$$x_\mu(E_\mu) = E_\mu/a.$$

For the muon mean energy $\langle E_\mu\rangle$ in the reaction $\nu_\mu + A \to \mu + X$, defining $\langle x_\mu\rangle$, we use the following [34,37] relationship:

$$\langle E_\mu\rangle = b \cdot E_{\nu_\mu}, \qquad b = \begin{cases} 0.5 & \text{for } \nu_\mu \\ 0.7 & \text{for } \bar{\nu}_\mu. \end{cases} \tag{19}$$

The neutrino mean free path is governed by the charged current (CC) interaction with nucleons. The corresponding cross section calculated in [38] can be approximated within ~10% accuracy as

$$\sigma_{\text{CC}} \approx \begin{cases} 0.72\times 10^{-36}\frac{E_{\nu_\mu}}{E_0}\,\text{cm}^2 & \text{for } \nu_\mu \\ 0.37\times 10^{-36}\frac{E_{\nu_\mu}}{E_0}\,\text{cm}^2 & \text{for } \bar{\nu}_\mu, \end{cases} \tag{20}$$

where $E_0 = 100$ GeV. For the respective mean free path, one has

$$x_{\nu_\mu} = \frac{1}{N_A\sigma_{\text{CC}}} \approx x_0\frac{E_0}{E_{\nu_\mu}}, \qquad x_0 \approx \begin{cases} 2.3\times 10^{12}\ \text{g/cm}^2 & \text{for } \nu_\mu \\ 4.5\times 10^{12}\ \text{g/cm}^2 & \text{for } \bar{\nu}_\mu, \end{cases} \tag{21}$$

where $N_A = 6\times 10^{23}$ 1/g is the number of nucleons per gram of matter. Separating annihilation neutrinos from different channels (ch) in Eq. (17), we have

$$\Phi_\mu = \frac{\dot{N}_{\text{ann}}}{8\pi r^2}\frac{b}{ax_0E_0}\sum_{\text{ch}}\text{Br}_{\text{ch}}N_{\nu_\mu(\text{ch})}\langle E^2_{\nu_\mu(\text{ch})}\rangle, \tag{22}$$

where Br_{ch}, $N_{\nu_\mu(\text{ch})}$, and $\langle E^2_{\nu_\mu(\text{ch})}\rangle$ are, respectively, the branching ratio, the neutrino yield, and the mean neutrino energy for a given channel. Equation (22) agrees numerically within 20% ÷ 40% with the respective formula of [34].

Figure 5 illustrates the difference in the most important N_2 annihilation channels for the cases of freeze-out (left panel) and solar core (right panel). Muon neutrinos produced in the channels $N_2N_2 \to \bar{u}u$, $\bar{d}d$, $\bar{s}s$, as well as in decays of any born muons, are not of interest because the primary particles have enough time to slow down before they decay, preventing neutrinos from producing a signal above the experimental threshold. Also, in the dense solar core, c and b quarks with initial energy $\gtrsim 100$ GeV partially lose their energy. However, we shall neglect this effect. It is not expected to cause an essential error, because, as we will show below, the muon signal is predicted to be virtually unobservable when highly energetic c and b quarks are born as a result of N_2 annihilation. In fact, for large N_2 mass, the $\bar{t}t$ and WW channels (see Fig. 5) dominate. Decaying, they give c and b quarks with degraded energy. So, a very large mass of N_2 is needed to noticeably produce highly energetic c and b quarks. However, for such masses, the muon signal is predicted to be small because of suppression of $\dot{N}_{\text{ann}}$ itself (in the model from [20]) and/or because of effects of ν_μ absorption in the solar matter. Generally, as seen in Eq. (22), in the absence of ν_μ absorption in matter, a decrease of neutrino energy quadratically reduces the intensity of the muon signal. For this reason, channels giving rise to ν_μ, as a result of a long cascade chain, can be considered negligible with respect to similar channels with shorter cascade chains of ν_μ production. Moreover, as a rule of thumb, longer chains have

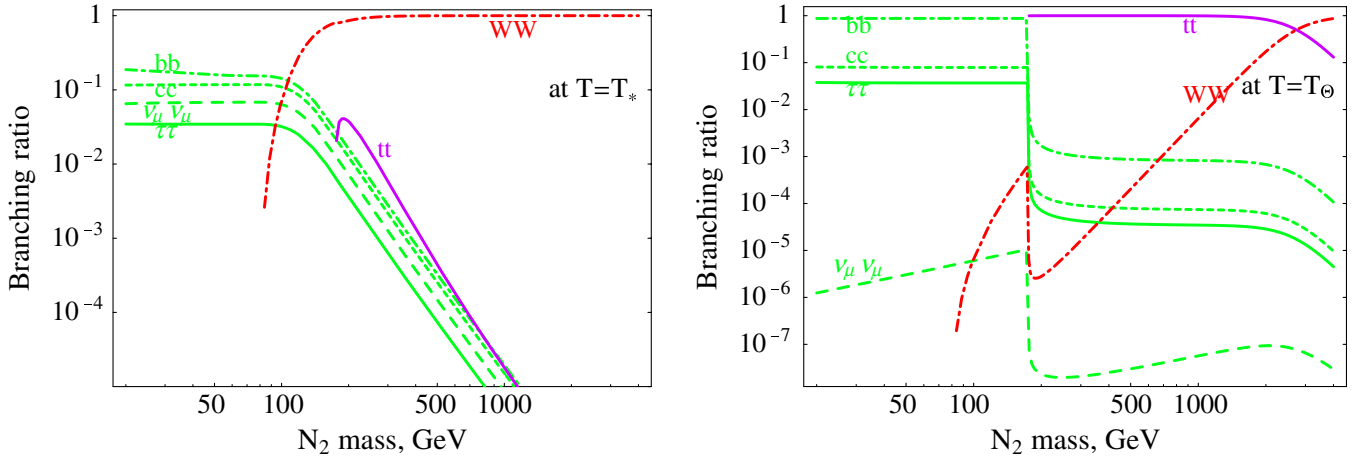

FIG. 5 (color online). The branching ratios of the most interesting N_2 annihilation channels for the cases of freeze-out (left panel) and in the solar core (right panel). The models from [20,24] do not differ in this plot.

an additional suppression due to the branching ratio. For example, the channels $N_2N_2 \to WW \to \tau\nu, bc, cs \to \nu_\mu X$ have a suppression with respect to $N_2N_2 \to WW \to \mu\nu_\mu \sim 10^2$ times.

We shall take into account the following channels:

$$N_2N_2 \to \nu_\mu \bar{\nu}_\mu, \tag{23}$$

$$N_2N_2 \to \tau^+\tau^- \to \mu\bar{\nu}_\mu\nu_\tau, \tag{24}$$

$$N_2N_2 \to c\bar{c} \to \mu\bar{\nu}_\mu X, \tag{25}$$

$$N_2N_2 \to b\bar{b} \to \mu\bar{\nu}_\mu X, \tag{26}$$

$$N_2N_2 \to W^+W^- \to \mu\bar{\nu}_\mu, \tag{27}$$

$$N_2N_2 \to t\bar{t} \to (W^- \to \mu\bar{\nu}_\mu)(\bar{b} \to \mu\bar{\nu}_\mu X), \tag{28}$$

where it is understood that we can have similar channels with the charge conjugate final states of the reactions above. The small branching ratio of the channel of Eq. (23), as Fig. 5 shows in the case of the Sun, is partially compensated by its short chain advantage mentioned above. The distributions of muonic neutrinos for energy $E_{\nu_\mu} \equiv E$ are given, correspondingly, for the channels of interest by

$$\frac{dN_{\nu_\mu}}{dE} = \delta(E - m) \quad \text{for Eq. (23)}, \tag{29}$$

$$\frac{dN_{\nu_\mu}}{dE} = \frac{0.18 \times 2}{m}\left[1 - 3\left(\frac{E}{m}\right)^2 + 2\left(\frac{E}{m}\right)^3\right]\eta(0, m) \quad \text{for Eq. (24)}, \tag{30}$$

$$\frac{dN_{\nu_\mu}}{dE} = \frac{0.13}{\bar{m}}\left[\frac{5}{3} - 3\left(\frac{E}{\bar{m}}\right)^2 + \frac{4}{3}\left(\frac{E}{\bar{m}}\right)^3\right]\eta(0, \bar{m}),$$
$$\bar{m} = 0.58m \quad \text{for Eq. (25)}, \tag{31}$$

$$\frac{dN_{\nu_\mu}}{dE} = \frac{0.103 \times 2}{\bar{m}}\left[1 - 3\left(\frac{E}{\bar{m}}\right)^2 + 2\left(\frac{E}{\bar{m}}\right)^3\right]\eta(0, \bar{m}),$$
$$\bar{m} = 0.73m \quad \text{for Eq. (26)}, \tag{32}$$

$$\frac{dN_{\nu_\mu}}{dE} = \frac{0.107}{m\beta}\eta\left(\frac{m}{2}(1 - \beta), \frac{m}{2}(1 + \beta)\right),$$
$$\beta = \sqrt{1 - \frac{m_W^2}{m^2}} \quad \text{for Eq. (27)}. \tag{33}$$

In the channel of Eq. (28), we have contributions from W and b decays:

$$\frac{dN_{\nu_\mu}}{dE} = \frac{dN_{\nu_\mu(W)}}{dE} + \frac{dN_{\nu_\mu(b)}}{dE} \quad \text{for Eq. (28)}, \tag{34}$$

$$\frac{dN_{\nu_\mu(W)}}{dE} = \frac{0.107}{(1 - \frac{m_W^2}{m_t^2})m\beta}\ln\left[\frac{\min(\frac{Em_t}{m(1-\beta)}, \frac{m_t}{2})}{\max(\frac{Em_t}{m(1+\beta)}, \frac{m_W^2}{2m_t})}\right]\eta\left(\frac{mm_W^2}{2m_t^2}(1 - \beta), \frac{m}{2}(1 + \beta)\right), \tag{35}$$

$$\frac{dN_{\nu_\mu(b)}}{dE} = \frac{0.103 \cdot 2}{(1 - \frac{m_W^2}{m_t^2})\bar{m}\beta}[F(E, E_-, E_+)\eta(0, E_-) + F(E, E, E_+)\eta(E_-, E_+)],$$
$$F(E, E_1, E_2) = \frac{2}{3}\left[\left(\frac{E}{E_1}\right)^3 - \left(\frac{E}{E_2}\right)^3\right] - \frac{3}{2}\left[\left(\frac{E}{E_1}\right)^2 - \left(\frac{E}{E_2}\right)^2\right] + \ln\frac{E_2}{E_1},$$
$$\bar{m} = 0.73m, \qquad E_\pm = \frac{m_t^2 - m_W^2}{2m_t}\bar{m}(1 \pm \beta),$$
$$\beta = \sqrt{1 - \frac{m_t^2}{m^2}}. \tag{36}$$

The step function is

$$\eta(E_1, E_2) \equiv \begin{cases} 1 & \text{for } E_1 < E < E_2, \\ 0 & \text{otherwise.} \end{cases}$$

Note that most of the formulas are taken from [34,39]. The values $\bar{m} < m$ in Eqs. (31), (32), and (36) take into account the partial energy losses by c and b quarks, respectively, while they are hadronized. For the WW channel, the effect of W polarization was neglected. Consideration of this effect would correct our estimation for ν_μ from this channel by ~20%. However, as we shall see, it is not necessary to consider this correction because for $m \gtrsim 3$ TeV, where the WW channel is important, the predicted muon signal becomes too faint for the existing experimental setups. Also note that the spectrum of Eq. (36) for ν_μ from b decay in Eq. (28) differs from that given in [34,39]. In the notation of [34,39], the signs before x^2 and y^2 in the respective formulas there should be altered in order to be correct. All spectra predicted by Eqs. (29)–(36) are illustrated in Fig. 6. The effect of absorption of ν_μ in solar matter is taken into account as follows [40]:

$$\frac{dN_{\nu_\mu}(\text{outside the Sun})}{dE} = \frac{dN_{\nu_\mu}(\text{in the solar core})}{dE} \times \exp\left(-\frac{E}{130\ \text{GeV}}\right), \tag{37}$$

$$\frac{dN_{\bar{\nu}_\mu}(\text{outside the Sun})}{dE} = \frac{dN_{\bar{\nu}_\mu}(\text{in the solar core})}{dE} \times \exp\left(-\frac{E}{200\ \text{GeV}}\right). \tag{38}$$

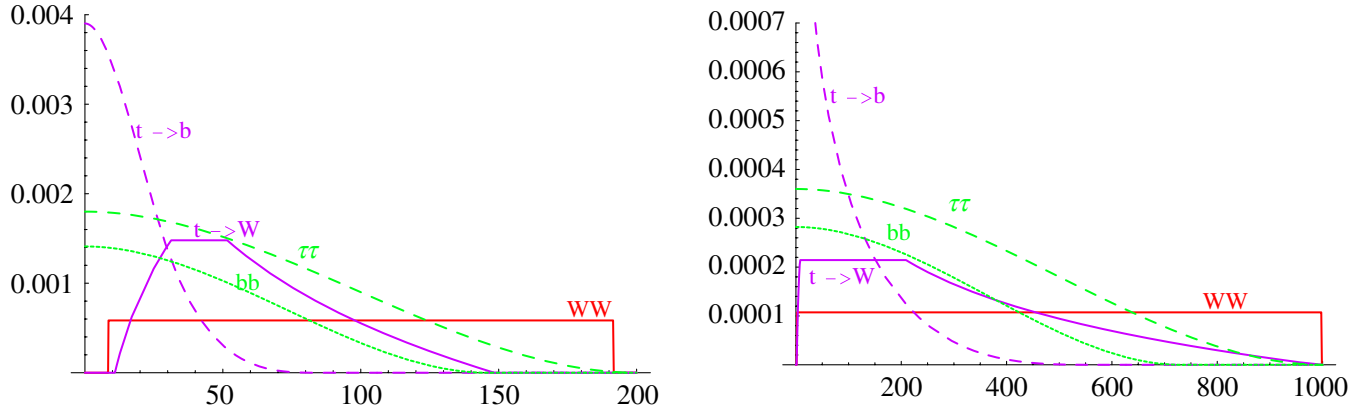

FIG. 6 (color online). The energy spectra of ν_μ produced in different channels for $m = 200$ GeV (left panel) and $m = 1000$ GeV (right panel).

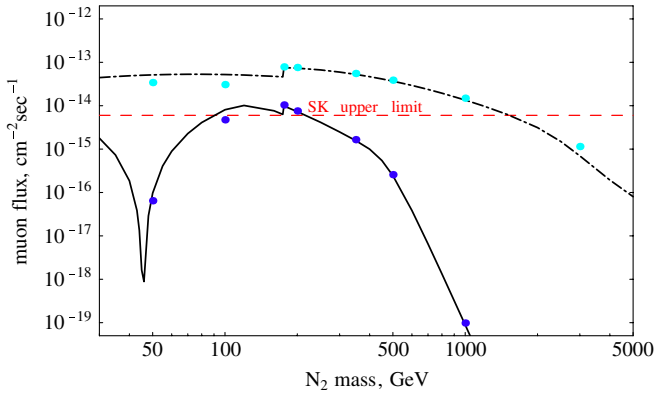

FIG. 7 (color online). Muon fluxes predicted for the models from [20] (solid line) and [24] (dot-dashed line) in comparison to the Super-Kamiokande constraint. Dark and light dots show predictions based on the results of [46] for the models from [20,24], respectively.

Note that the spectra in the solar core for neutrinos ν_μ and antineutrinos $\bar{\nu}_\mu$ do not differ and are given by Eqs. (29) and (31)–(36).

The muon (including both μ^- and μ^+) fluxes predicted for the models from [20,24] are shown in Fig. 7. We compare them with the respective upper limit obtained by the Super-Kamiokande Collaboration [41],

$$\Phi_\mu < 6 \times 10^{-15}\ \mathrm{cm}^{-2}\,\mathrm{s}^{-1}.$$

It relates to an angle of 10° around the solar center, which is expected to embrace most of the muon flux induced by annihilation in the Sun for the N_2 masses of interest. For our chosen parameters, the SK limit excludes the intervals

$$100\ \mathrm{GeV} < m < 200\ \mathrm{GeV} \tag{39}$$

for the model from [20] and

$$m < 1500\ \mathrm{GeV} \tag{40}$$

for the model from [24].

V. DISCUSSION

In the present paper we have considered candidates emerging from the minimal walking technicolor model with a suppressed coupling to the Z boson. These candidates can account for the dark matter density of the Universe and can simultaneously avoid any contradiction with the results of direct dark matter search experiments. In fact, CDMS and Xenon experiments can exclude only a tiny window around 100 GeV for the model from [20]. Being elusive for direct dark matter searches, we investigated the possibility of indirect effects of N_2 dark matter particles. In particular, we estimated the neutrino fluxes on the surface of the Earth from N_2 annihilations in the Sun and in the Earth. These effects can provide constraints on the parameters of the considered models.

One of the biggest uncertainties entering these constraints is that the final results depend on the local density of DM particles as well as on the velocity distribution. As one can see in Fig. 7, a decrease of ρ_{loc} down to 0.2 GeV/cm^3, a value that is currently acceptable, with unchanged velocity distribution, would leave only a tiny interval of m around 110 GeV excluded for the model from [20]. This makes any conclusion for the model from [20] indefinite, based on the searches for muon signals. In any case, the obtained constraint is more strict than the one based on direct dark matter search experiments [22].

Regarding the model from [24], the existing uncertainties can hardly influence essentially the excluded range of Eq. (40). This result agrees with the analogous result, obtained by the Kamiokande Collaboration for Majorana neutrinos [42], although it differs in some details (which are most likely related to the estimations of cross sections for different annihilation channels and their neutrino yields). Moreover, the effects of b and c quarks slowing down in dense solar matter (which are neglected in our consideration) and all the unaccounted for annihilation chains (which produce ν_μ, including chains which go through b and c quarks) can lead to an increase in the

predicted muon fluxes for large m. This can give neutrinos with lower energy, which may avoid absorption in solar matter. For this reason, the channel $N_2N_2 \to \bar{t}t \to b \to \nu_\mu X$, giving softer ν_μ than ν_μ from $t \to W$ and WW channels (see Fig. 6), has a significant contribution for high m.

Uncertainties also come from neutrino propagation effects, i.e. neutrino oscillations and interactions with matter. Oscillation effects in vacuum and matter [43] might change the flavor content of the neutrino flux going from the solar core to the detectors on the Earth. The uncertainties in the description of oscillations become less ambiguous once we average the effect because of the large distance, energy, and time measurement intervals involved. Indeed, neutrinos of three flavors are generated in the source. The flux of muon neutrinos at the Earth is

$$\Phi_{\nu_\mu} = P_{\mu\mu}\Phi_{\nu_\mu} + P_{e\mu}\Phi_{\nu_e} + P_{\tau\mu}\Phi_{\nu_\tau}, \qquad (41)$$

where $P_{\alpha\beta}$ is the probability of transition between flavors α and β. As we see in the right panel of Fig. 5, the most important N_2 annihilation channels of neutrino production, depending on the mass, are $N_2N_2 \to \bar{b}b$ with b decaying into $cl\bar{\nu}$, $N_2N_2 \to \bar{t}t$ with $t \to Wb$, and $N_2N_2 \to WW$ with $W \to l\bar{\nu}$. In order to give a simple estimate of the effect of neutrino oscillations, we are going to consider the $\bar{b}b$ mode as the dominant one for $m < 200$ GeV, the $\bar{t}t$ mode for $0.2 < m < 3$ TeV, and the WW mode for $m > 3$ TeV. In the $\bar{b}b$ mode, the production of ν_τ is suppressed because of the fact that τ is much heavier than the muon and the electron (we ignore here the difference in the neutrino spectra, and we also ignore the production of ν_τ from τ decay), so the produced neutrino flux is roughly $\nu_e + \nu_\mu + 0.3\nu_\tau$. In the WW mode, one has $\nu_e + \nu_\mu + \nu_\tau$. Finally, in the $\bar{t}t$ mode both W and b decay, so we have roughly $\nu_e + \nu_\mu + 0.7\nu_\tau$. For the transition probabilities obtained in [44], within the three-flavor scheme, we have the following: all $P_{\alpha\beta} \approx 0.3$ for $E \lesssim 10$ GeV, and $P_{\mu\mu} = P_{\tau\mu} = P_{\tau\tau} \approx 0.4$, $P_{\tau e} = P_{\mu e} \approx 0.2$, and $P_{ee} \approx 0.6$ for $E \gg 10$ GeV. Therefore, the following change of the flavor content of the neutrino flux going from the solar core to the detector might take place,

$$\nu_e + \nu_\mu + 0.3\nu_\tau \Rightarrow \begin{cases} 0.8\nu_e + 0.8\nu_\mu + 0.8\nu_\tau, & \text{at } E \lesssim 10 \text{ GeV} \\ 0.9\nu_e + 0.7\nu_\mu + 0.7\nu_\tau, & \text{at } E \gg 10 \text{ GeV,} \end{cases} \quad \text{for } m \lesssim 200 \text{ GeV,}$$

$$\nu_e + \nu_\mu + 0.7\nu_\tau \Rightarrow 0.9\nu_e + 0.9\nu_\mu + 0.9\nu_\tau, \quad \text{at any } E, \quad \text{for } 200 \text{ GeV} \lesssim m \lesssim 3 \text{ TeV,}$$

$$\nu_e + \nu_\mu + \nu_\tau \Rightarrow \nu_e + \nu_\mu + \nu_\tau, \quad \text{at any } E, \quad \text{for } m \gtrsim 3 \text{ TeV.}$$

In our rough estimate we assume that $P_{\alpha\beta} = P_{\beta\alpha} = (P_{\alpha\beta} + P_{\bar{\alpha}\bar{\beta}})/2$. In this simplified picture we see that oscillations redistribute the flavor content of the neutrino flux, making it more homogenous. This would decrease the predicted ν_μ flux by ~20%.

Effects of ν interactions lead not only to absorption of neutrinos in solar matter due to CC interactions, but also to a loss of energy for $\nu_{e,\mu}$ due to neutral current (NC) interactions, and for ν_τ due to both NC and CC (in the latter case ν_τ is regenerated from the chain $\nu_\tau N \to \tau X$, $\tau \to \nu_\tau X$). Energy loss is a small effect (the ratio of respective cross sections is $\sigma_{\rm NC}/\sigma_{\rm CC} \sim 1/3$). It should decrease the muon signal a little for small m, but increase it a bit for large m. This is analogous to the neutrinos produced from the long cascade chains that we neglected, since a shift to a lower energy partially saves neutrinos from absorption.

In the four-flavor oscillation scheme, where a sterile type of neutrino ν_s is added, there can also be a damping effect of the signal for low N_2 mass, because of the $\nu_\mu \to \nu_s$ transition. However, an amplification of the signal for high mass can occur because of the larger penetrating ability of neutrinos oscillating to ν_s [45].

In [46] (including the website referred to therein), the muon fluxes for separate annihilation channels are obtained, taking into account oscillation and interaction effects. For the sake of comparison, we have taken their data on muon fluxes for the case of "standard" oscillation parameters (case "B" in their notation). For a mass $m <$ 175 GeV we considered the channels $b\bar{b}$, $c\bar{c}$, $\tau\tau$, for $175 < m < 2000$ GeV the $t\bar{t}$ channel, and for $m > 2000$ GeV the $t\bar{t}$ and WW ones. Since the data were related to muon fluxes per one annihilation act, we multiplied the fluxes by the respective annihilation rates. The points on Fig. 7 show the respective results for a few mass values. As seen, the agreement is extremely good, especially for high N_2 mass. Therefore, the upper limits on m in Eqs. (39) and (40) do not change appreciably. At lower mass (which is of limited interest for the models studied), where the $b\bar{b}$ channel dominates, a slightly larger difference is noted between our result and [46], mainly due to ignorance of the b-quark energy losses in our calculation and the aforementioned oscillation effect. However, the suppression of ν_μ yields from the $b\bar{b}$ channel is partially compensated by the excessive ν_μ yields from the $\tau\tau$ channel scaling as 4% of the branching ratio at this particular mass range. As it is

shown in Fig. 7, the difference between our calculation and that of [46] is practically indistinguishable on the plot.

ACKNOWLEDGMENTS

The work of K. B. was supported by Khalatnikov-Starobinsky Leading Scientific School Grant No. N 4899.2008.2 and Russian Leading Scientific School Grant No. N 3489.2008.2. The work of C. K. was supported by the Marie Curie Fellowship under Contract No. MEIF-CT-2006-039211. We would also like to thank J. Edsjö for helping with the interpretation of the results published in [46].

[1] S. Weinberg, Phys. Rev. D **19**, 1277 (1979).
[2] L. Susskind, Phys. Rev. D **20**, 2610 (1979).
[3] F. Sannino and K. Tuominen, Phys. Rev. D **71**, 051901 (2005).
[4] D. K. Hong, S. D. H. Hsu, and F. Sannino, Phys. Lett. B **597**, 89 (2004).
[5] D. D. Dietrich, F. Sannino, and K. Tuominen, Phys. Rev. D **72**, 055001 (2005).
[6] D. D. Dietrich and F. Sannino, Phys. Rev. D **75**, 085018 (2007).
[7] S. Catterall and F. Sannino, Phys. Rev. D **76**, 034504 (2007).
[8] L. Del Debbio, M. T. Frandsen, H. Panagopoulos, and F. Sannino, J. High Energy Phys. 06 (2008) 007.
[9] L. Del Debbio, A. Patella, and C. Pica, arXiv:0805.2058.
[10] S. B. Gudnason, C. Kouvaris, and F. Sannino, Phys. Rev. D **73**, 115003 (2006).
[11] R. Foadi, M. T. Frandsen, T. A. Ryttov, and F. Sannino, Phys. Rev. D **76**, 055005 (2007).
[12] A. Belyaev, R. Foadi, M. T. Frandsen, M. Jarvinen, A. Pukhov, and F. Sannino, Phys. Rev. D **79**, 035006 (2009).
[13] D. D. Dietrich and C. Kouvaris, Phys. Rev. D **78**, 055005 (2008).
[14] D. D. Dietrich and C. Kouvaris, arXiv:0809.1324 [Phys. Rev. D (to be published)].
[15] S. B. Gudnason, C. Kouvaris, and F. Sannino, Phys. Rev. D **74**, 095008 (2006).
[16] T. A. Ryttov and F. Sannino, Phys. Rev. D **78**, 115010 (2008).
[17] M. Y. Khlopov and C. Kouvaris, Phys. Rev. D **77**, 065002 (2008).
[18] M. Y. Khlopov and C. Kouvaris, Phys. Rev. D **78**, 065040 (2008).
[19] M. Y. Khlopov, arXiv:0806.3581.
[20] C. Kouvaris, Phys. Rev. D **76**, 015011 (2007).
[21] R. Bernabei *et al.*, Riv. Nuovo Cimento Soc. Ital. Fis. **26N1**, 1 (2003); Eur. Phys. J. C **56**, 333 (2008).
[22] C. Kouvaris, Phys. Rev. D **78**, 075024 (2008).
[23] C. Kouvaris, Phys. Rev. D **77**, 023006 (2008).
[24] K. Kainulainen, K. Tuominen, and J. Virkajarvi, Phys. Rev. D **75**, 085003 (2007).
[25] E. Kolb and K. Olive, Phys. Rev. A **33**, 1202 (1986).
[26] T. K. Gaisser *et al.*, Phys. Rev. D **34**, 2206 (1986).
[27] M. Joyce, Phys. Rev. D **55**, 1875 (1997).
[28] J. Lewin and P. Smith, Astropart. Phys. **6**, 87 (1996).
[29] J. Ellis *et al.*, Phys. Lett. B **481**, 304 (2000).
[30] K. Belotsky, M. Khlopov, and K. Shibaev, Phys. At. Nucl. **65**, 382 (2002); Part. Nucl. Lett. **108**, 5 (2001).
[31] K. Belotsky and M. Khlopov, Grav. and Cosmol. **11**, 220 (2005).
[32] D. Hooper and J. Silk, New J. Phys. **6**, 23 (2004).
[33] A. Gould, Astrophys. J. **388**, 338 (1992).
[34] G. Jungman, M. Kamionkowski, and K. Griest, Phys. Rep. **267**, 195 (1996).
[35] T. Damour and L. Krauss, Phys. Rev. D **59**, 063509 (1999); L. Bergstrom *et al.*, J. High Energy Phys. 08 (1999) 010; K. M. Belotsky, T. Damour, and M. Yu. Khlopov, Phys. Lett. B **529**, 10 (2002); A. Gould and S. M. K. Alam, Astrophys. J. **549**, 72 (2001).
[36] W.-M. Yao *et al.*, Review of Particle Physics, J. Phys. G **33**, 1 (2006).
[37] S. Ritz and D. Seckel, Nucl. Phys. **B304**, 877 (1988).
[38] R. Gandhi *et al.*, Phys. Rev. D **58**, 093009 (1998).
[39] D. Hooper and G. Servant, Astropart. Phys. **24**, 231 (2005).
[40] P. Crotty, Phys. Rev. D **66**, 063504 (2002).
[41] H. Nishino *et al.* (Super-Kamiokande Collaboration), Phys. Rev. D **70**, 083523 (2004).
[42] M. Mori *et al.* (Kamiokande Collaboration), Phys. Lett. B **289**, 463 (1992).
[43] L. Wolfenstein, Phys. Rev. D **17**, 2369 (1978); S. P. Mikheev and A. Yu. Smirnov, Yad. Fiz. **42**, 1441 (1985) [Sov. J. Nucl. Phys. **42**, 913 (1985)].
[44] M. Cirelli *et al.*, Nucl. Phys. **B727**, 99 (2005).
[45] V. Naumov, Phys. Lett. B **529**, 199 (2002).
[46] M. Blennow, J. Edsjö, and T. Ohlsson, J. Cosmol. Astropart. Phys. 01 (2008) 021; the authors results can be found at www.physto.se/edsjo/wimpsim.